Mon. Not. R. Astron. Soc. **000**, 000–000 (0000) Printed 24 November 2011 (MN LATEX style file v2.2)

Refined physical properties of the HAT-P-13 planetary system

John Southworth [1], I. Bruni [2], L. Mancini [3], J. Gregorio [4]
[1] *Astrophysics Group, Keele University, Newcastle-under-Lyme, ST5 5BG, UK*
[2] *INAF – Osservatorio Astronomico di Bologna, Via Ranzani 1, 40127 Bologna, Italy*
[3] *Max Planck Institute for Astronomy, Königstuhl 17, 69117 – Heidelberg, Germany*
[4] *Grupo Atalaia, CROW Observatory-Portalegre, Portugal*

24 November 2011

ABSTRACT
We present photometry of four transits of the planetary system HAT-P-13, obtained using defocussed telescopes. We analyse these, plus nine datasets from the literature, in order to determine the physical properties of the system. The mass and radius of the star are $M_{\rm A} = 1.320 \pm 0.048 \pm 0.039\,{\rm M}_{\odot}$ and $R_{\rm A} = 1.756 \pm 0.043 \pm 0.017\,{\rm R}_{\odot}$ (statistical and systematic errorbars). We find the equivalent quantities for the transiting planet to be $M_{\rm b} = 0.906 \pm 0.024 \pm 0.018\,{\rm M}_{\rm Jup}$ and $R_{\rm b} = 1.487 \pm 0.038 \pm 0.015\,{\rm R}_{\rm Jup}$, with an equilibrium temperature of $T'_{\rm eq} = 1725 \pm 31$ K. Compared to previous results, which were based on much sparser photometric data, we find the star to be more massive and evolved, and the planet to be larger, hotter and more rarefied. The properties of the planet are not matched by standard models of irradiated gas giants. Its large radius anomaly is in line with the observation that the hottest planets are the most inflated, but at odds with the suggestion of inverse proportionality to the $\left[\frac{\rm Fe}{\rm H}\right]$ of the parent star. We assemble all available times of transit midpoint and determine a new linear ephemeris. Previous findings of transit timing variations in the HAT-P-13 system are shown to disagree with these measurements, and can be attributed to small-number statistics.

Key words: stars: planetary systems — stars: fundamental parameters — stars: individual: HAT-P-13

1 INTRODUCTION

The discovery of the HAT-P-13 by Bakos et al. (2009) elicited substantial interest. The transiting extrasolar planet (TEP) HAT-P-13 b and its host star HAT-P-13 A are rather typical examples of these objects, with two exceptions. Firstly, the star is the second-most metal-rich known to host a TEP after XO-2 A[1] (Burke et al. 2007) (but see the discussion on host star $\left[\frac{\rm Fe}{\rm H}\right]$ values in Enoch et al. 2011). Secondly, there is a third component in the system which is clearly detected in the radial velocity measurements (RVs) of the host star (Bakos et al. 2009). HAT-P-13 c has an orbit with a period of 446.22 ± 0.27 d, an eccentricity of 0.6616 ± 0.0052 and a minimum mass of $14.28 \pm 0.28\,{\rm M}_{\rm Jup}$ (Winn et al. 2010b). This object is expected to induce transit timing variations (TTVs) within the HAT-P-13 A,b system, which potentially allow the structure of the planet to be probed (Mardling & Lin 2004; Batygin et al. 2009). HAT-P-13 is unfortunately not the best system for such analyses, as its relatively long and shallow transits are not conducive to precise timing measurements.

An observation of the Rossiter-McLaughlin effect by Winn et al. (2010b) has shown that the projected angle between the orbital axis of HAT-P-13 b and the rotational axis of the parent star is consistent with zero. This is in line with the fact that misaligned axes are only found for TEP systems containing a star hotter than roughly 6250 K (Winn et al. 2010a; Schlaufman 2010; Albrecht et al. 2011). Winn et al. (2010b) also found a long-term drift in the radial velocity measurements of the star, which may be the signature of a *fourth* component to the system on an orbit of much longer period.

Szabó et al. (2010) attempted to detect a transit of the third body, at a time predicted by Winn et al. (2010b), but were not successful. Their observational campaign included scrutiny of two transits of HAT-P-13 b, whose times of occurrence agreed well with the predicted timings. Pál et al. (2011) subsequently presented photometry of three transits, all of whose midpoints fell earlier than expected according to an ephemeris built on the observations of Bakos et al. (2009) and Szabó et al. (2010). Pál et al. interpreted this as evidence of TTVs. Nascimbeni et al. (2011b) presented high-speed photometry of five transits in early 2011, taken as part of the TASTE project (Nascimbeni et al. 2011a). They confirmed that a linear ephemeris could not explain the available transit timings, and postulated that a sinusoidal TTV with an amplitude of 0.005 d was a good match to the available transit timings. Sinusoidal TTVs have previously been seen for WASP-3 (Pollacco et al. 2008; Maciejewski et al. 2010) and WASP-10 (Christian et al. 2009; Maciejewski

[1] See: `http://www.astro.keele.ac.uk/∼jkt/tepcat/`

Table 1. Log of the observations presented in this work. $N_{\rm obs}$ is the number of observations and 'Moon illum.' is the fractional illumination of the Moon at the midpoint of the transit. The aperture sizes are the radii of the software apertures for the object, inner sky and outer sky, respectively.

Transit	Date	Start time (UT)	End time (UT)	$N_{\rm obs}$	Exposure time (s)	Filter	Airmass	Moon illum.	Aperture sizes (px)	Scatter (mmag)
Cassini	2011 02 06	19:21	00:37	127	120	Thuan-Gunn i	$1.17 \rightarrow 1.00 \rightarrow 1.10$	0.129	25, 35, 55	0.77
Cassini	2011 04 17	18:58	23:50	147	90	Thuan-Gunn i	$1.03 \rightarrow 2.11$	0.998	18, 30, 50	0.93
Portalegre	2011 01 31	22:13	05:21	128	180	Cousins I	$1.11 \rightarrow 1.01 \rightarrow 1.64$	0.041	10, 35, 45	2.47
Portalegre	2011 02 03	20:53	02:55	119	150	Cousins I	$1.25 \rightarrow 1.01 \rightarrow 1.16$	0.008	10, 35, 45	2.53

Table 2. Excerpts of the light curves of HAT-P-13. The full dataset will be made available at the CDS.

Telescope	BJD(TDB)	Diff. mag.	Uncertainty
Cassini	2455599.30664	0.00061	0.00090
Cassini	2455599.52535	−0.00085	0.00078
Cassini	2455669.29046	−0.00014	0.00108
Cassini	2455669.49355	0.00066	0.00117
Portalegre	2455593.43105	−2.08860	0.00250
Portalegre	2455593.72843	−2.09700	0.00270
Portalegre	2455596.37600	−0.55520	0.00270
Portalegre	2455596.62736	−0.54600	0.00260

et al. 2011) but have not yet been confirmed[2]. The putative TTVs for HAT-P-13 have been challenged by Fulton et al. (2011), who presented observations of ten transits over two observing seasons. They found that a linear ephemeris was an acceptable match to all transit timing measurements, with the exception of the first of the two obtained by Szabó et al. (2010).

The physical properties of the HAT-P-13 system have been derived by Bakos et al. (2009) and Winn et al. (2010b), who used the same light curves. Since these studies a wealth of new photometric data has been gathered. This has been used to investigate putative TTVs, but has not been brought to bear on improving the physical properties of the system. In this work we present new photometry covering four transits and use all available high-quality photometry to measure refined physical properties of HAT-P-13.

2 OBSERVATIONS AND DATA REDUCTION

Two full transits of HAT-P-13 were observed with the BFOSC imager mounted on the 1.52 m G. D. Cassini Telescope[3] at Loiano Observatory, Italy. We used a Gunn i filter and autoguided throughout. We had to reject a small number of datapoints in both transits, as they were affected by pointing jumps which compromised the data quality. A summary of our observations is given in Table 1 and the full data can be found in Table 2.

The telescope was defocussed so the point spread functions (PSFs) resembled annuli of widths 15–25 pixels, in order to reduce the light from the target and comparison stars to a maximum of roughly 35 000 counts per pixel. This approach reduces the susceptibility of the data to flat-fielding noise and increases the efficiency of the observations. A detailed description of the defocussing method can be found in Southworth et al. (2009a,b), and an instance of its use with the Cassini telescope in Southworth et al. (2010). Several images were taken with the telescope properly focussed, and used to verify that there were no faint stars within the defocussed PSF of HAT-P-13.

Data reduction was undertaken using standard methods pertaining to aperture photometry. Software aperture positions were specified by hand but shifted to account for pointing variations, which were found by cross-correlating each image against the reference image used to place the apertures. We found that the results were insensitive to the choice of aperture sizes (within reason)

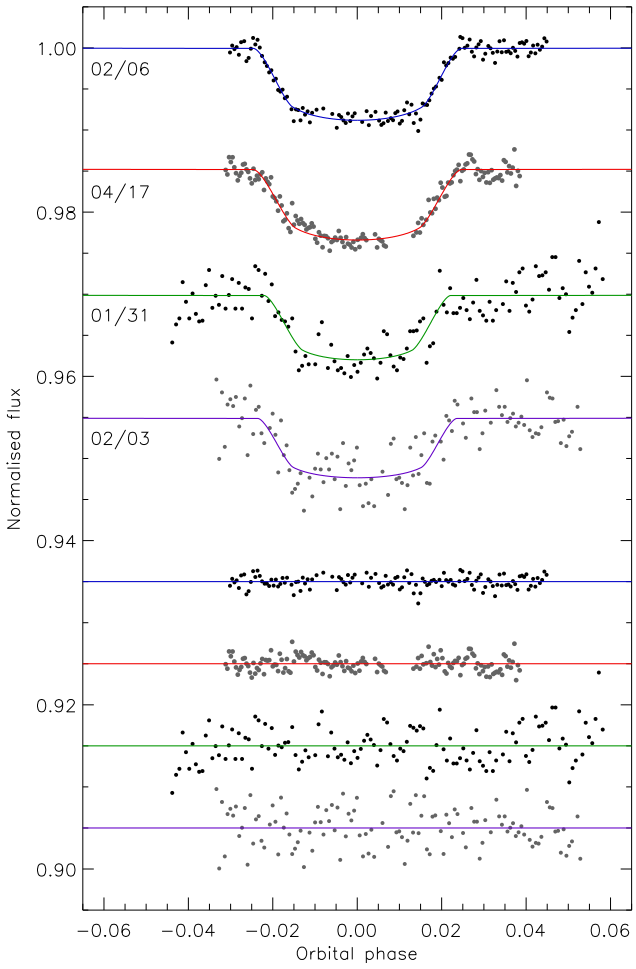

Figure 1. New data presented in this work, compared to the best JKTEBOP fits using the quadratic LD law. The dates of the light curves are labelled using the format month/day. The residuals of the fits are plotted in the lower half of the figure, offset from zero.

[2] A sinusoidal TTV was claimed for OGLE-TR-111 by Díaz et al. (2008) but has been refuted by Adams et al. (2010)

[3] Information on the 1.52 m Cassini Telescope and BFOSC can be found at `http://www.bo.astro.it/loiano/`

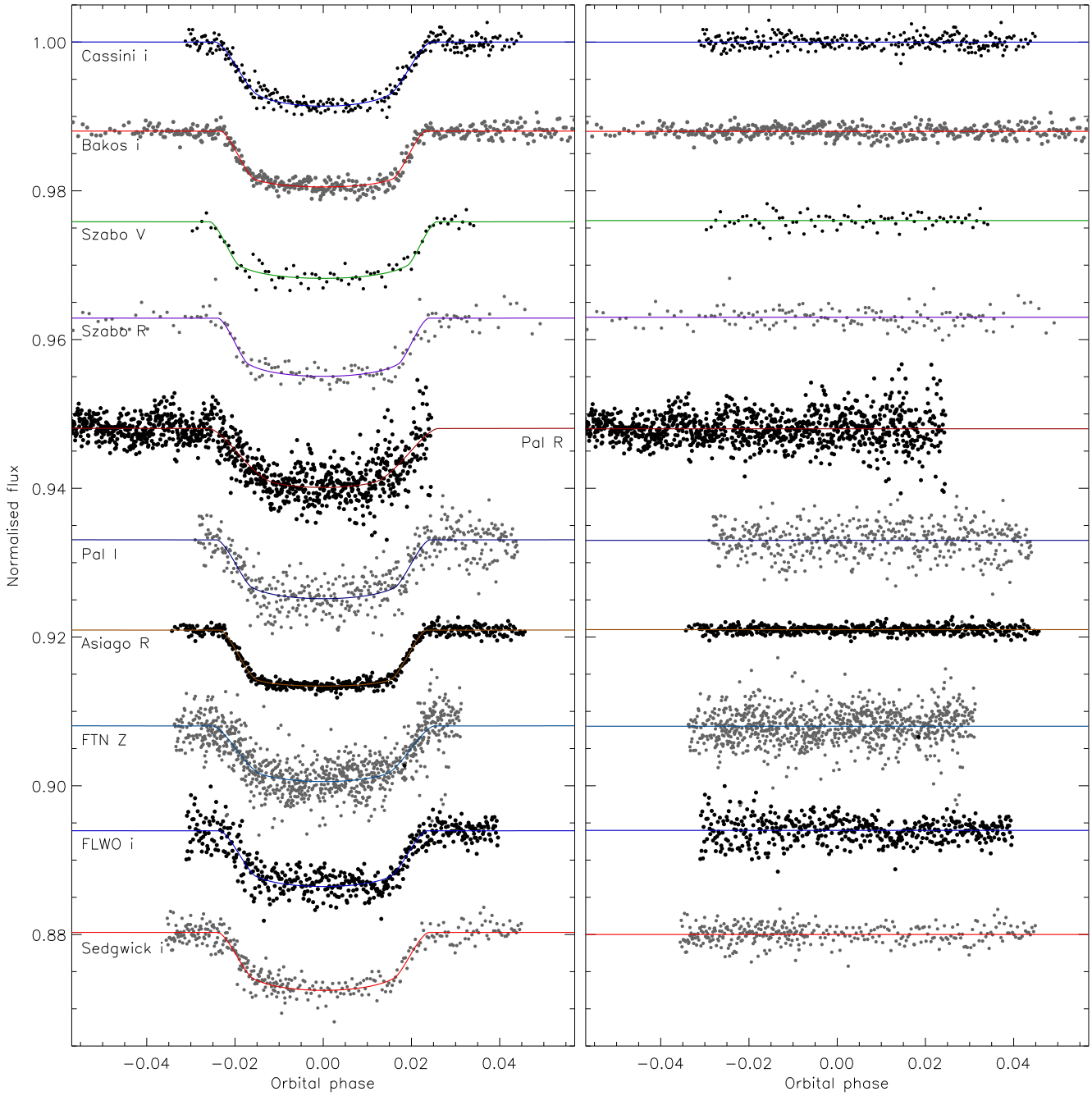

Figure 2. Phased light curves of HAT-P-13 compared to the best JKTEBOP fits using the quadratic LD law (left panel). They are shown in the same order as in Table 3. The residuals of the fits are plotted in the right panel, offset to bring them into the same relative position as the corresponding best fit in the left panel.

and to whether flat fields were used in the data reduction process. Differential-photometry light curves were obtained with respect to an optimal ensemble of four comparison stars constructed as outlined by Southworth et al. (2009a). The times of observation were converted to barycentric Julian date on the TDB timescale, using the IDL procedures of Eastman et al. (2010).

Two full transits were observed by JG from CROW-Portalegre, Portugal, using an f/5.6 30 cm Schmidt-Cassegrain telescope, a KAF1603 CCD camera operating at a plate scale of $1.12''$ px^{-1}, and a Cousins I filter. The data were reduced by standard methods, using median-combined bias, dark and flat-field calibration observations. Aperture photometry was performed with C-Munipack[4] and differential-magnitude light curves obtained with respect to an ensemble of five comparison stars.

3 LIGHT CURVE ANALYSIS

We have analysed the Cassini and literature photometric observations of HAT-P-13 by the methods of the *Homogeneous Studies*

[4] http://c-munipack.sourceforge.net/

Table 3. Parameters of the JKTEBOP fits to the light curves of HAT-P-13. The final parameters correspond to the weighted mean of the results for the ten light curves.

Source	$r_{\rm A}+r_{\rm b}$	k	i (°)	$r_{\rm A}$	$r_{\rm b}$
Cassini i-band	0.211 ± 0.014	0.0932 ± 0.0015	81.6 ± 1.0	0.193 ± 0.013	0.0180 ± 0.0014
Bakos FLWO i-band	0.193 ± 0.011	0.08592 ± 0.00084	82.61 ± 0.87	0.178 ± 0.010	0.0153 ± 0.0010
Szabó V-band	0.192 ± 0.030	0.0836 ± 0.0046	83.8 ± 3.2	0.178 ± 0.028	0.0148 ± 0.0031
Szabó R-band	0.207 ± 0.024	0.0872 ± 0.0026	81.7 ± 1.8	0.190 ± 0.022	0.0165 ± 0.0019
Pál R-band	0.217 ± 0.034	0.0895 ± 0.0073	81.5 ± 2.6	0.200 ± 0.031	0.0178 ± 0.0036
Pál I-band	0.210 ± 0.019	0.0887 ± 0.0032	81.5 ± 1.3	0.193 ± 0.017	0.0171 ± 0.0018
Nascimbeni R-band	0.2103 ± 0.0048	0.08668 ± 0.00052	81.97 ± 0.36	0.1852 ± 0.0044	0.01606 ± 0.00042
Fulton FTN Z-band	0.231 ± 0.023	0.0882 ± 0.0041	80.2 ± 1.6	0.212 ± 0.021	0.0187 ± 0.0021
Fulton FLWO i-band	0.208 ± 0.016	0.0868 ± 0.0023	81.5 ± 1.2	0.191 ± 0.015	0.0166 ± 0.0017
Fulton Sedgwick i-band	0.199 ± 0.017	0.0873 ± 0.0029	82.4 ± 1.4	0.183 ± 0.016	0.0159 ± 0.0017
Final results			$\mathbf{81.93 \pm 0.26}$	$\mathbf{0.1863 \pm 0.0034}$	$\mathbf{0.01622 \pm 0.00034}$
Bakos et al. (2009)	0.1856	0.0844 ± 0.0013	83.4 ± 0.6	0.1712 ± 0.0076	0.01445
Winn et al. (2010b)	0.1839	0.08389 ± 0.00081	83.40 ± 0.68	0.1697 ± 0.0072	0.01424
Fulton et al. (2011)	0.1967	0.0855 ± 0.0011	82.45 ± 0.46	0.1812 ± 0.0056	0.01549

project (Southworth 2008, 2009, 2010, 2011), which are briefly summarised below. The light curves and their best-fitting models are shown in Fig. 1 for the data presented in this paper, and in Fig. 2 for previously published observations. The ensuing parameters of the fit are given in Table 3 and detailed results for each dataset can be found in an online-only supplement. The Portalegre transits were analysed using the same methods, but only the transit times are used below due to the comparatively large scatter of these data.

The light curves were modelled using the JKTEBOP[5] code. The primary fitted parameters were the sum and ratio of the fractional radii of the star and planet, $r_{\rm A}+r_{\rm b}$ and $k = \frac{r_{\rm b}}{r_{\rm A}}$, and the orbital inclination, i. The fractional radii of the components are defined as $r_{\rm A} = \frac{R_{\rm A}}{a}$ and $r_{\rm b} = \frac{R_{\rm b}}{a}$ where a is the orbital semimajor axis, and $R_{\rm A}$ and $R_{\rm b}$ are the true radii of the two objects. Additional parameters of the fit included the magnitude level outside transit and the midpoint of the transit.

We generated solutions with each of five limb darkening (LD) laws (linear, quadratic, square-root, logarithmic and cubic), and with three different treatments of the LD coefficients. The first possibility is to fix both coefficients to values predicted using model atmospheres; this leads to a dependence on stellar theory as well as slightly worse fits due to the larger number of degrees of freedom. The second option is to fit for both coefficients, but this is possible only when the data are of extremely high quality. Unless otherwise stated, we go for a third alternative: fit for the linear LD coefficients and fix the nonlinear one to theoretically predicted values ('LD-fit/fix' in the nomenclature of Southworth 2010). The two coefficients are highly correlated (e.g. Southworth et al. 2007a) so the theoretical dependence inherent in this approach is negligible.

Uncertainties in each solution were calculated in two ways: from 1000 Monte Carlo (MC) simulations (Southworth et al. 2004), and with a residual-permutation (RP) algorithm (Jenkins et al. 2002). The larger of the two possible errorbars was retained for each fitted parameter. Orbital eccentricity (e) and periastron longitude (ω) were incorporated using the constraints $e\cos\omega = -0.0099 \pm 0.0036$ and $e\sin\omega = -0.0060 \pm 0.0069$ (Winn et al. 2010b). These constraints were treated as observational data and $e\cos\omega$ and $e\sin\omega$ were included as fitted parameters.

[5] JKTEBOP is written in FORTRAN77 and the source code is available at `http://www.astro.keele.ac.uk/~jkt/`

3.1 Analysis of each dataset

The two Cassini transits were modelled together, after scaling the observational errors for each transit to give a reduced χ^2 of $\chi^2_\nu = 1.0$. This step is necessary because the errors returned by the aperture photometry routine we use are usually too small. Due to the possibility of TTVs in the HAT-P-13 system one has to be careful when combining data. In this case we fitted for the orbital period ($P_{\rm orb}$) and the midpoint of the first transit, which is equivalent to fitting for the two transit midpoints. The RP errorbars were selected because they are larger than the MC ones. The LD-fit/fix results were adopted. A final value for each photometric parameter was obtained by taking the weighted mean of the four values from the fits for the non-linear LD laws. Its errorbar was taken to be the largest of the four alternative values, with a contribution added in quadrature to account for any dependence of the parameter value on the choice of LD law.

Bakos et al. (2009) presented i-band data obtained with the 1.2 m telescope and KeplerCam at the F. L. Whipple Observatory (FLWO). The 3719 datapoints extend over seven transits within an interval of approximately one year, but only two of these transits have full phase coverage. We therefore converted the timestamps into orbital phase (using the ephemeris calculated by Fulton et al. 2011), sorted them and combined each set of eight consecutive points, to obtain 466 phase-binned points. This will wash out any TTVs present over that time interval, but inspection of fig. 7 in Bakos et al. (2009) shows that no significant variations exist. A preliminary fit returned $\chi^2_\nu = 7.53$ so the errorbars were scaled up by $\sqrt{7.53}$. The LD-fit/fix results are adopted and combined as above. The RP errors were larger than the MC ones, which is unusual for phase-binned data (Southworth 2011) but accounted for in our analysis.

Szabó et al. (2010) obtained V- and R-band coverage of two transits; we did not consider the V-band data of the second transit as it suffers from systematic errors. The R-band observations were solved with $P_{\rm orb}$ as a fitted parameter, so the solutions are not sensitive to the effects of putative TTVs. Given the limited quantity of the data we did not attempt LD-fitted solutions. In both cases we found that correlated noise was unimportant and adopted the LD-fit/fix solutions. The T_0 values from the two datasets (referenced to cycle -12) are in poor agreement with each other (see Tables A3 and A4), and roughly bracket the time of midpoint derived by

Szabó et al. (2010). All three timings deviate from the ephemeris derived below by much more than the derived uncertainties.

Pál et al. (2011) presented photometry of three transits from two telescopes located at Konkoly Observatory. The first transit was obtained with the Schmidt telescope and a CCD camera equipped with a Bessell I filter. The second and third came from the 1.0 m telescope with VersArray CCD camera and a Cousins R filter. The two datasets were modelled separately after scaling up their errorbars to enforce $\chi^2_\nu = 1.0$. For both bands we adopted the LD-fit/fix solutions. The MC errorbars are larger than the RP ones, indicating that red noise is not important.

The data presented by Nascimbeni et al. (2011b) were obtained with the Asiago 1.82 m telescope and AFOSC imager, through a Cousins R filter. They comprise 12 585 observations covering five closely adjacent transits with cadences ranging from 5.8 s to 9.7 s. The data were taken over only 38 days, so can be combined without suffering smearing effects due to TTVs with periodicities above several months. We therefore phase-binned them by a factor of 25 into 504 bins, during which process a 4σ clip removed 11 of the observations. A preliminary fit returned $\chi^2_\nu = 1.07$ so the supplied observational errors were left unmodified. The results show a strong preference for weaker LD than theoretical expectations, and the values for r_A and r_b depend somewhat on the treatment of LD. The LD-fixed solutions can be rejected due to a lower quality of fit, and the LD-fitted equivalents return unphysical coefficients, so the LD-fit/fix alternatives were adopted. RP errors are smaller than MC ones, as we ordinarily find for phase-binned data.

Fulton et al. (2011) obtained photometry of ten transits of HAT-P-13, of which only four were fully covered. These include two transits taken just over a year apart using the Faulkes Telescope North (FTN) and a Z filter, which were solved with a free P_orb to allow for the possibility of TTVs. A third transit was obtained in the i band with the FLWO 1.2 m. Finally, one i-band transit from the Sedgwick 0.8 m is accompanied by a partial transit obtained only three nights earlier, allowing these data to be modelled with P_orb fixed to any reasonable value. We found that the errorbars of the Sedgwick and FTN data had to be multiplied by $\sqrt{8.05}$ and $\sqrt{5.35}$, respectively, to obtain $\chi^2_\nu = 1.0$. For the FTN and Sedgwick data we were able to adopt the LD-fit/fix solutions, but for FLWO had to stick to LD-fixed as attempts to fit for LD coefficients returned unphysical values. For the FTN and FLWO data the RP errors are moderately larger than those from the MC algorithm, implying that correlated noise is significant in these light curves.

Table 4. Times of minimum light of HAT-P-13 and their residuals versus the ephemeris derived in this work.

Time of minimum BJD(TDB) − 2400000	Cycle no.	Residual (JD)	Reference
54581.62443 ± 0.00122	−204.0	−0.00183	Bakos et al. (2009)
54777.01324 ± 0.00100	−137.0	−0.00099	Bakos et al. (2009)
54779.92990 ± 0.00063	−136.0	−0.00057	Bakos et al. (2009)
54782.84394 ± 0.00155	−135.0	−0.00277	Bakos et al. (2009)
54849.92099 ± 0.00075	−112.0	0.00080	Bakos et al. (2009)
54882.00078 ± 0.00150	−101.0	0.00197	Bakos et al. (2009)
54960.74005 ± 0.00178	−74.0	0.00281	Bakos et al. (2009)
55167.79647 ± 0.00280	−3.0	0.00631	Gary(AXA)
55194.03566 ± 0.00229	6.0	−0.00065	Fulton et al. (2011)
55196.95450 ± 0.00127	7.0	0.00195	Fulton et al. (2011)
55199.86837 ± 0.00123	8.0	−0.00041	Tieman(TRESCA)
55199.86867 ± 0.00131	8.0	−0.00011	Fulton et al. (2011)
55231.94542 ± 0.00091	19.0	−0.00199	Fulton et al. (2011)
55249.45117 ± 0.00200	25.0	0.00634	Szabó et al. (2010)
55269.86567 ± 0.00180	32.0	0.00717	Gary(AXA)
55272.77577 ± 0.00120	33.0	0.00103	Gary(AXA)
55272.77627 ± 0.00250	33.0	0.00153	Foote(AXA)
55275.69207 ± 0.00180	34.0	0.00109	Gary(AXA)
55275.69312 ± 0.00266	34.0	0.00214	Fulton et al. (2011)
55307.77077 ± 0.00370	45.0	0.00117	Gary(AXA)
55310.69197 ± 0.00250	46.0	0.00613	Gary(AXA)
55511.90854 ± 0.00141	115.0	0.00226	Fulton et al. (2011)
55558.56302 ± 0.00098	131.0	−0.00307	Pál et al. (2011)
55561.48416 ± 0.00400	132.0	0.00183	Pál et al. (2011)
55564.39876 ± 0.00180	133.0	0.00019	Nascimbeni et al. (2011b)
55584.81455 ± 0.00153	140.0	0.00231	Dvorak(TRESCA)
55590.64523 ± 0.00179	142.0	0.00052	Pál et al. (2011)
55593.55879 ± 0.00185	143.0	−0.00216	This work (Portalegre)
55593.56147 ± 0.00115	143.0	0.00052	Nascimbeni et al. (2011b)
55596.47291 ± 0.00140	144.0	−0.00428	Naves(TRESCA)
55596.47327 ± 0.00202	144.0	−0.00392	This work (Portalegre)
55596.47662 ± 0.00305	144.0	−0.00057	Nascimbeni et al. (2011b)
55599.39267 ± 0.00075	145.0	−0.00076	Nascimbeni et al. (2011b)
55599.39446 ± 0.00100	145.0	0.00103	This work (Cassini)
55602.31068 ± 0.00167	146.0	0.00101	Nascimbeni et al. (2011b)
55613.97390 ± 0.00225	150.0	−0.00072	Fulton et al. (2011)
55616.89290 ± 0.00152	151.0	0.00204	Fulton et al. (2011)
55619.80786 ± 0.00134	152.0	0.00076	Fulton et al. (2011)
55622.72351 ± 0.00166	153.0	0.00018	Fulton et al. (2011)
55669.38140 ± 0.00126	169.0	−0.00175	This work (Cassini)

3.2 Combined results

The photometric parameters resulting from the ten light curves are collected in Table 3. We calculated the weighted means to obtain final values of these quantities. The χ^2_ν values of the averaging process are all below 0.5, with the exception of k. We deduce that the ten light curves are in sufficient mutual agreement. The final values are dominated by the results from the Asiago light curve, which is easily the best of the available datasets.

For k the averaging process yields $\chi^2_\nu = 2.0$, so the agreement between the light curve solutions is not so good. The Cassini data are the primary contributor to this situation, as they point to a larger k than the rest of the datasets. Individual solutions of the two Cassini light curves yield similar values of k. Moderate disagreements in k have been frequently seen in the *Homogeneous Studies* papers and can be attributed to starspot activity and/or systematic errors in the light curve. k is also determined to a high precision (by comparison to r_A, r_b and i) so systematic differences are comparatively obvious.

Our final photometric parameters (Table 3) are somewhat different to values based on the discovery photometry (Bakos et al. 2009; Winn et al. 2010b). In particular we find a lower i and larger r_A. The latter quantity is observationally strongly tied to r_b so our results point towards a larger star and planet than previously proposed. Our photometric parameters agree reasonably well with those proposed recently by Fulton et al. (2011), but have smaller uncertainties.

4 ON THE TRANSIT TIMINGS OF HAT-P-13 B

The third body in the HAT-P-13 system, known to have an eccentric orbit with $e_\mathrm{c} = 0.6616 \pm 0.0052$ and $P_{\mathrm{orb,c}} = 446.22 \pm 0.27$ d from radial velocity measurements, is expected to cause TTVs within the inner HAT-P-13 A,b system (Bakos et al. 2009; Payne

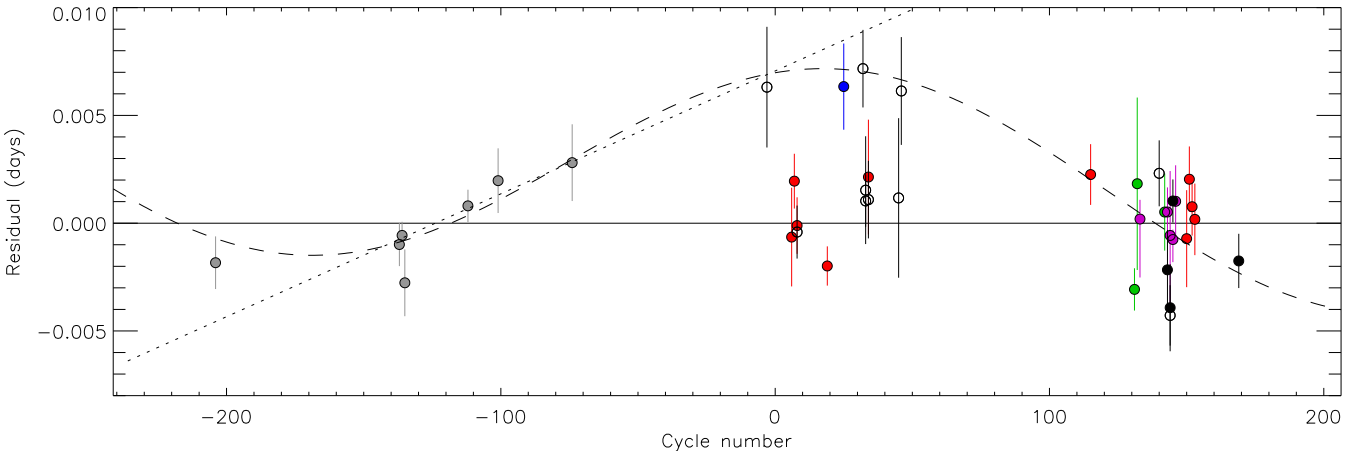

Figure 3. Plot of the residuals of the timings of mid-transit of HAT-P-13 versus a linear ephemeris. The timings in black are from this work, in grey are from Bakos et al. (2009), blue from Szabó et al. (2010), lilac from Pál et al. (2011), green from Nascimbeni et al. (2011b), red from Fulton et al. (2011), and open circles for the amateur timings. The solid line shows the ephemeris from the current work and the dotted line that from Bakos et al. (2009). The dashed curve is an approximate representation of the possible periodicity proposed by Nascimbeni et al. (2011b).

& Ford 2011). Bakos et al. found "suggestive" but not "significant" evidence for TTVs in their data obtained in their 2007-8 and 2008-9 observing seasons. Szabó et al. (2010) obtained an improved orbital ephemeris and placed an upper limit of 0.001 d on size of the phenomenon, with the inclusion of their two transit times from the 2009-10 season.

However, the times of three transits acquired by Pál et al. (2011) during the 2010-11 season were about 22 minutes early with respect to the previous orbital ephemerides, leading Pál et al. to claim a significant detection of TTVs. The timings found by Pál et al. were supported by Nascimbeni et al. (2011b) on the basis of five new transits obtained during the same observing season. Nascimbeni et al. demonstrated that a sinusoidal TTV function provided a good fit to all existing timing measurements.

Fulton et al. (2011) have subsequently presented ten transit timings which cast doubt on the possibility of TTVs: five from the 2010-11 season which agree well with those from Pál et al. (2011) and Nascimbeni et al. (2011b), and five from the previous season which conflict with the timings found by Szabó et al. (2010). Fulton et al. reanalysed all published follow-up observations of HAT-P-13 and concluded that they were consistent with a linear ephemeris with the exception of the first transit dataset from Szabó et al. (2010).

In order to firmly establish the character of the situation, we have collected all available transit midpoint times for the HAT-P-13 A,b system. We have used the timings as quoted by the original sources, rather than adopting those from the reanalysis by Fulton et al. (2011). We included ten timings obtained by amateur astronomers and placed on the AXA[6] and TRESCA[7] websites. We rejected amateur timings which are based on data that are either very scattered or do not cover a full transit.

Transit timings were obtained from our own observations by fitting JKTEBOP models to each transit following the LD-fit/fix prescription. The flux normalisation was allowed to vary linearly with time. Errors were estimated from RP and from 1000 MC simulations, and were multiplied by two in order to guard against any undetected systematic noise in the data. At the request of the referee we also assessed correlated noise using the 'β' approach (e.g. Winn et al. 2007). We evaluated values for individual transits and for groups of between two and ten datapoints, finding a maximum β of 1.26. The corresponding increases in the uncertainties in the T_0 values are smaller than the factor of two we used above.

All timings were placed on the BJD(TDB) time system. We fitted a straight line to obtain a new orbital ephemeris, finding $\chi^2_\nu = 2.00$ with one obvious outlier. After the rejection of the offending point, which is the first timing from Szabó et al. (2010), we obtained:

$$T_0 = \mathrm{BJD(TDB)}\ 2\,455\,176.53878(27) + 2.9162383(22) \times E$$

with $\chi^2_\nu = 1.54$. The bracketed quantities represent the uncertainties in the ephemeris, and have been increased to account for the excess χ^2_ν. The full list of transit timings and their references is given in Table 4. It should be noted that many of the timings are measured from data covering only part of a transit, which is known to reduce their reliability (e.g. Gibson et al. 2009).

The two timings from Szabó et al. (2010) both deviate from the orbital ephemeris above, being later by 8.6σ and 3.2σ. Our own analyses of these data return timings which are similarly distant from expectations. A detailed reanalysis of the corresponding data performed by Fulton et al. (2011) resulted in a timing for the second of these transits which conflicts less with a linear ephemeris (1.6σ). The discrepancy of the first transit remains unexplained. A few of the amateur timings are late by a similar amount to this one, but with much larger errorbars.

We conclude that the available data do not provide a clear indication of the existence of TTVs, primarily on the basis that we cannot conceive of a reasonable TTV function which is a significant improvement over a linear ephemeris. The transits which occur later than predicted by our ephemeris are not grouped together, but are interleaved with ones which happen at the expected times. An explanation involving TTVs therefore would require a highly contrived functional form.

So where did the previous suggestions of TTVs come from? Pál et al. (2011) used an earlier ephemeris, tuned on the Bakos et al. (2009) and Szabó et al. (2010) observations, to show that their transit timings were earlier than expected. The dotted line in

[6] Amateur Exoplanet Archive, `http://brucegary.net/AXA/x.htm`
[7] The TRansiting ExoplanetS and CAndidates (TRESCA) website can be found at, `http://var2.astro.cz/EN/tresca/index.php`

Table 5. Final physical properties of the HAT-P-13 system, compared with results from the literature. Where two errorbars are given, the first refers to the statistical uncertainties and the second to the systematic errors.

	This work (final)	Bakos et al. (2009)	Winn et al. (2010b)
$M_{\rm A}$ ($\mathrm{M}_\odot$)	$1.320 \pm 0.048 \pm 0.039$	$1.219^{+0.050}_{-0.099}$	$1.22^{+0.05}_{-0.10}$
$R_{\rm A}$ ($\mathrm{R}_\odot$)	$1.756 \pm 0.043 \pm 0.017$	1.559 ± 0.082	1.559 ± 0.080
$\log g_{\rm A}$ (cgs)	$4.070 \pm 0.020 \pm 0.004$	4.13 ± 0.04	
$\rho_{\rm A}$ ($\rho_\odot$)	0.244 ± 0.013		
$M_{\rm b}$ ($\mathrm{M}_{\rm Jup}$)	$0.906 \pm 0.024 \pm 0.018$	$0.853^{+0.029}_{-0.046}$	0.851 ± 0.038
$R_{\rm b}$ ($\mathrm{R}_{\rm Jup}$)	$1.487 \pm 0.038 \pm 0.015$	1.281 ± 0.079	1.272 ± 0.065
$g_{\rm b}$ ($\mathrm{m\,s^{-1}}$)	10.15 ± 0.43	12.9 ± 1.5	
$\rho_{\rm b}$ ($\rho_{\rm Jup}$)	$0.257 \pm 0.017 \pm 0.003$	$0.375^{+0.078}_{-0.052}$	
$T'_{\rm eq}$ (K)	1725 ± 31	1653 ± 45	
Θ	$0.0404 \pm 0.0023 \pm 0.0004$	0.046 ± 0.003	
a (AU)	$0.04383 \pm 0.00053 \pm 0.00043$	$0.0427^{+0.0006}_{-0.0012}$	
Age (Gyr)	$3.5\,^{+1.1\ +0.3}_{-2.9\ -0.7}$	$5.0^{+2.5}_{-0.8}$	

Fig. 3 represents this ephemeris and shows that it fails to match the more recent transit timings. Nascimbeni et al. (2011b) suggested that a sinusoidal TTV of amplitude 0.005 d and period 1150 d was in good correspondance with the observations, as demonstrated by their fig. 2. We have endeavoured to place this periodic variation, whose parameters were not fully specified, onto Fig. 3, with a little manual fine-tuning. The 2009-10 transit timings obtained by Fulton et al. (2011) clearly dismiss the sinusoidal TTV proposed by Nascimbeni et al. (2011b), leaving a linear ephemeris as the only reasonable option.

5 PHYSICAL PROPERTIES OF THE HAT-P-13 SYSTEM

Several sets of information exist from which the properties of the HAT-P-13 A,b system can be derived. Analysis of the available light curves has given values for $P_{\rm orb}$, i, $r_{\rm A}$ and $r_{\rm b}$. The high-precision radial velocities procured by Bakos et al. (2009) and Winn et al. (2010b) supply measurements of the velocity amplitude of the star ($K_{\rm A} = 106.04 \pm 0.73\,\mathrm{m\,s^{-1}}$) and the orbital eccentricity ($e = 0.0133 \pm 0.0041$). Analysis of the spectra by Bakos et al. (2009) furthermore lead to estimates of the stellar effective temperature ($T_{\rm eff} = 5653 \pm 90$ K) and metallicity ($\left[\frac{\rm Fe}{\rm H}\right] = +0.41 \pm 0.08$). Finally, constraints on the properties of the star can be obtained by interpolation within tabulated predictions from stellar evolutionary models.

Our solution process (Southworth 2009) consists of finding the best agreement between the observed and model-predicted $T_{\rm eff}$s, and the measured $r_{\rm A}$ and calculated $\frac{R_{\rm A}}{a}$. This is done using the velocity amplitude of the planet, $K_{\rm b}$, as a solution control parameter and calculating the full system properties using standard formulae (e.g. Hilditch 2001). The system properties comprise the mass, radius, surface gravity and mean density for the star ($M_{\rm A}$, $R_{\rm A}$, $\log g_{\rm A}$ and $\rho_{\rm A}$) and planet ($M_{\rm b}$, $R_{\rm b}$, $g_{\rm b}$ and $\rho_{\rm b}$), the orbital semimajor axis (a), the planetary equilibrium temperature and Safronov (1972) number ($T'_{\rm eq}$, Θ) and an estimate of the evolutionary age of the star.

The statistical errors on the resulting values are calculated using a perturbation analysis (Southworth et al. 2005) which yields a full error budget for each output quantity. The use of theoretical models incurs a dependence on stellar theory which is assessed by running separate solutions with each of five different sets of model tabulations (see Southworth 2010 for details). Finally, an alternative empirical estimate of the physical properties is obtained using a calibration (Southworth 2011) based on eclipsing binary star systems, inspired by Enoch et al. (2010) and Torres et al. (2010). The control parameter $K_{\rm b}$ represents the constraints obtained from stellar theory. Note that the values $g_{\rm b}$, $\rho_{\rm A}$ and $T'_{\rm eq}$ are not reliant on constraints from stellar theory (Southworth et al. 2007b; Seager & Mallén-Ornelas 2003; Southworth 2011).

The sets of physical properties arising from each of the five stellar model tabulations and from the empirical calibration are given in Table A11. For the final results in Table 5 we adopted the unweighted mean of each parameter from the solutions for the five stellar models. The statistical error is the largest of the individual errorbars, and the systematic error is the standard deviation of the five values. Compared to previous studies, we find a larger and more evolved star and a correspondingly slightly more massive but significantly bigger and hotter planet. The extensive photometric dataset considered in this work leads to more precise measurements of the physical properties, but the uncertainties in $r_{\rm A}$ and $r_{\rm b}$ continue to dominate the error budget. The uncertainty in $M_{\rm A}$ stems mainly from that in $\left[\frac{\rm Fe}{\rm H}\right]$, suggesting that a new spectral synthesis study would also be useful in improving our understanding of the HAT-P-13 system.

6 SUMMARY

The HAT-P-13 system is unusual in that a transiting hot Jupiter and its host star are accompanied by a clearly-detected third component on a wider orbit. Such a configuration should result in HAT-P-13 c inducing TTVs within the HAT-P-13 A,b system, which may be detectable within a comparatively short time period. This possibility has generated substantial interest, resulting in a large body of photometric observations covering many transits of the star by the inner planet. We have assembled the available transit timing measurements and shown that they are most easily explained by a linear ephemeris, albeit with a small number of values which occur later than expected. The discrepant measurements are not clumped together, so could only be explained via highly complex functional forms. Previous claims of TTVs can be attributed to small-number statistics, although continued photometric monitoring has a good chance of turning up something interesting in the future.

We have presented new observations of four transits, obtained using telescope defocussing techniques. Including previously published data, we have ten good sets of transit light curves. These

were each analysed within the context of our *Homogeneous Studies* project (Southworth 2008, 2009, 2010, 2011), and a good agreement between the results was found. We combined them with the measured spectroscopic properties of the host star and several sets of theoretical stellar model predictions to find the physical properties of the system. HAT-P-13 is now well-characterised, although additional photometric and spectroscopic measurements would allow further improvement. We have included it in the TEPCat catalogue[8] of the physical properties of transiting planetary systems.

We find a significantly different set of physical properties compared to previous studies, which had access to only two of the ten photometric datasets used here. The star is more massive, larger and more evolved. The planet, whose properties are measured relative to its host star, is similarly heavier and bigger. Its lower density and higher equilibrium temperature place it firmly in the 'pM' class advocated by Fortney et al. (2008). Its radius is too large to match the values predicted by the models of Fortney et al. (2007) or Baraffe et al. (2008).

Laughlin et al. (2011) found that the radius anomaly (the measured radius of a TEP versus that predicted by theoretical models) is correlated with equilibrium temperature, and possibly inversely correlated with host star $\left[\frac{\rm Fe}{\rm H}\right]$. The large radius anomaly and high equilibrium temperature of HAT-P-13 b corroborate the former observation, but the highly metal-rich nature of the parent star ($\left[\frac{\rm Fe}{\rm H}\right] = 0.41 \pm 0.08$) is contrary to the latter suggestion.

ACKNOWLEDGMENTS

The reduced light curves presented in this work will be made available at the CDS (`http://cdsweb.u-strasbg.fr/`) and at `http://www.astro.keele.ac.uk/~jkt/`. This observational campaign has been possible thanks to the generous allocation of telescope time by the TAC of the Bologna Observatory and to the invaluable help of the technical staff. JS acknowledges financial support from STFC in the form of an Advanced Fellowship. We thank Andras Pál for supplying photometric data and the anonymous referee for insightful comments. The following internet-based resources were used in research for this paper: the ESO Digitized Sky Survey; the NASA Astrophysics Data System; the SIMBAD database operated at CDS, Strasbourg, France; and the arχiv scientific paper preprint service operated by Cornell University.

REFERENCES

Adams, E. R., López-Morales, M., Elliot, J. L., Seager, S., Osip, D. J., 2010, ApJ, 714, 13
Albrecht, S., et al., 2011, ApJ, 738, 50
Bakos, G. Á., et al., 2009, ApJ, 707, 446
Baraffe, I., Chabrier, G., Barman, T., 2008, A&A, 482, 315
Batygin, K., Bodenheimer, P., Laughlin, G., 2009, ApJ, 704, L49
Burke, C. J., et al., 2007, ApJ, 671, 2115
Christian, D. J., et al., 2009, MNRAS, 392, 1585
Díaz, R. F., Rojo, P., Melita, M., Hoyer, S., Minniti, D., Mauas, P. J. D., Ruíz, M. T., 2008, ApJ, 682, L49
Eastman, J., Siverd, R., Gaudi, B. S., 2010, PASP, 122, 935
Enoch, B., Collier Cameron, A., Parley, N. R., Hebb, L., 2010, A&A, 516, A33
Enoch, B., et al., 2011, AJ, 142, 86
Fortney, J. J., Marley, M. S., Barnes, J. W., 2007, ApJ, 659, 1661
Fortney, J. J., Lodders, K., Marley, M. S., Freedman, R. S., 2008, ApJ, 678, 1419
Fulton, B. J., Shporer, A., Winn, J. N., Holman, M. J., Pál, A., Gazak, J. Z., 2011, AJ, 142, 84
Gibson, N. P., et al., 2009, ApJ, 700, 1078
Hilditch, R. W., 2001, An Introduction to Close Binary Stars, Cambridge University Press, Cambridge, UK
Jenkins, J. M., Caldwell, D. A., Borucki, W. J., 2002, ApJ, 564, 495
Laughlin, G., Crismani, M., Adams, F. C., 2011, ApJ, 729, L7
Maciejewski, G., et al., 2010, MNRAS, 407, 2625
Maciejewski, G., et al., 2011, MNRAS, 411, 1204
Mardling, R. A., Lin, D. N. C., 2004, ApJ, 614, 955
Nascimbeni, V., Piotto, G., Bedin, L. R., Damasso, M., 2011a, A&A, 527, A85
Nascimbeni, V., Piotto, G., Bedin, L. R., Damasso, M., Malavolta, L., Borsato, L., 2011b, A&A, 532, A24
Pál, A., Sárneczky, K., Szabó, G. M., Szing, A., Kiss, L. L., Mező, G., Regály, Z., 2011, MNRAS, 413, L43
Payne, M. J., Ford, E. B., 2011, ApJ, 729, 98
Pollacco, D., et al., 2008, MNRAS, 385, 1576
Safronov, V. S., 1972, Evolution of the Protoplanetary Cloud and Formation of the Earth and Planets (Jerusalem: Israel Program for Scientific Translation)
Schlaufman, K. C., 2010, ApJ, 719, 602
Seager, S., Mallén-Ornelas, G., 2003, ApJ, 585, 1038
Southworth, J., 2008, MNRAS, 386, 1644
Southworth, J., 2009, MNRAS, 394, 272
Southworth, J., 2010, MNRAS, 408, 1689
Southworth, J., 2011, MNRAS, 417, 2166
Southworth, J., Maxted, P. F. L., Smalley, B., 2004, MNRAS, 351, 1277
Southworth, J., Maxted, P. F. L., Smalley, B., 2005, A&A, 429, 645
Southworth, J., Bruntt, H., Buzasi, D. L., 2007a, A&A, 467, 1215
Southworth, J., Wheatley, P. J., Sams, G., 2007b, MNRAS, 379, L11
Southworth, J., et al., 2009a, MNRAS, 396, 1023
Southworth, J., et al., 2009b, MNRAS, 399, 287
Southworth, J., et al., 2010, MNRAS, 408, 1680
Szabó, G. M., et al., 2010, A&A, 523, A84
Torres, G., Andersen, J., Giménez, A., 2010, A&ARv, 18, 67
Winn, J. N., Fabrycky, D., Albrecht, S., Johnson, J. A., 2010a, ApJ, 718, L145
Winn, J. N., et al., 2007, AJ, 134, 1707
Winn, J. N., et al., 2010b, ApJ, 718, 575

[8] The **T**ransiting **E**xtrasolar **P**lanets **Cat**alogue can be found online at `http://www.astro.keele.ac.uk/~jkt/tepcat/`